Tracking and Mitigation of Chirp-Type Interference in GPS Receivers Using Adaptive Notch Filters

Arif, S., Coskun, A. and Kale, I.

Tracking and Mitigation of Chirp-Type Interference in GPS Receivers Using Adaptive Notch Filters

Syed Waqas Arif, Adem Coskun and Izzet Kale
Applied DSP and VLSI Research Group Department of Engineering, University of Westminster
waqas.arif@my.westminster.ac.uk, a.coskun@westminster.ac.uk, kalei@westminster.ac.uk

***Abstract*—A Global Positioning System (GPS) receiver is extremely prone to intentional and unintentional interference due to weak signal power experienced on the surface of the earth, which severely affects the navigation functionality and occasionally avoids the receivers from acquiring the GPS signal. This work presents a comparative performance analysis of two different types of Adaptive Notch Filtering (ANF) algorithms for GPS specific applications that are (1) Direct form 2nd Order ANF and (2) Lattice-based ANF for tracking and mitigation of Chirp-type Interference. Three classes of chirp-type interference signals, studied in this paper, are linear chirp, quadratic chirp and cubic chirp. Performance of each ANF algorithm is evaluated at the output of the acquisition module in terms of search-grid SNR and Peak metric.**

Keywords—Interference, Adaptive Notch Filter, GPS receivers, Chirp Interference.

I. INTRODUCTION

Global Positioning System (GPS) is in existence for more than four decades. It is most widely used satellite positioning constellation among the existing Global Navigation Satellite Systems (GNSS), while commercial multi-constellation GNSS receivers have gained popularity in only recent years. GPS provides world-wide coverage which makes it the most favourable constellation for research and development of satellite-based navigation and positioning receivers. Navigation signals transmitted by GNSS are modulated using Direct Sequence Spread Spectrum (DSSS) techniques which provides built-in robustness to interference but only to some extent. The power level of the received GPS signal at receiver's RF front end is in the order of 10^{-16} Watts and it is 20 dB below the thermal noise experienced at the receiver. Due to the extremely low received signal power level, the GNSS receivers are vulnerable to slighted of the interference in the in-band region of the useful signal spectrum. This effect of the interferer on the useful signal is very evident across the Cross Ambiguity Function (CAF) observed at the early stages of acquisition process. Abnormities caused by interference ripple through other operational blocks within the receiver, hence completely dysfunction receiver's ability to provide accurate Positioning, Velocity and Timing (PVT) information. Considering the low GNSS signal power at the receiver, there is an increasing need for an appropriate interference mitigation technique that is cost-effective and at the same time preserving the useful GNSS signal. Different types of interference affect the GNSS signal in different ways, hence distorting Corse-Acquisition (CA) code and CAF in the correlation process differently. There are numerous interference mitigation techniques which involve direct excision of interference signal based on Time-Frequency (TF) plane (such as adaptive frequency-domain filtering [1] and Time-Frequency Domain (TFD) [2] filtering). The drawback of these techniques is that high computational load, which in turn increases the hardware complexity of the GPS receivers despite the limited hardware resources and power available on-board. Various ANF algorithms have been implemented for interference suppression [3-5], however, most of the research focuses on excision of narrowband Continuous Wave Interference (CWI). ANF based techniques provide a cost effective solution due to their low complexity and computational load [6] and proven to be very effective in excision of unwanted signal in the GNSS signals spectrum. Hence, ANF based algorithms have become very lucrative in the sense that they only require the update of two filter coefficients to realize a second-order Infinite Impulse Response (IIR) filter. In more challenging scenarios, the jamming/interference signal's instantaneous frequency sweeps a range of several megahertz in few microseconds and corrupts the entire GPS band. Such jamming signal is known as Chirp Signal (swept-frequency) and can be classified as linear-chirp, quadratic-chirp or cubic-chirp. The research work in [7] and [8] demonstrate the excision of linear swept frequency chirp interference effectively via ANF using Auto-Regressive Moving-Average (ARMA) configuration. However, analysis of different ANF algorithms for tracking and mitigation of linear and quadratic-chirp and within GNSS receivers is still far from being fully covered and this research addresses mitigation of other types of chirp interferences via lattice based ANF and Direct Form second IIR ANF to enrich and broaden the investigation. This paper is divided into five sections. Section II describes the modelling of the signals and system within an acquisition module. Section III discusses ANF algorithms based on the adaptation of notch center frequency. Section IV demonstrates a set of simulation based results. Finally Section V summarizes the findings and serves as a conclusion section.

II. SIGNAL AND SYSTEMMODEL

In this section the chirp-type interference and the GPS signal models are formulated along with the performance metrics used for this paper.

A. Chirp Interferences

A chirp signal is characterize by instantaneous variations of carrier frequency over frequency bandwidth known as sweep bandwidth B_c over one chirp period T_c sweep period of chirp.

$$j_{chirp}[n] = \sqrt{2P_c}\cos\underbrace{(2\pi f_o nT_s + 2\pi u_c (nT_s)^2/2 + \emptyset_c)}_{\theta[n]} \quad (1)$$

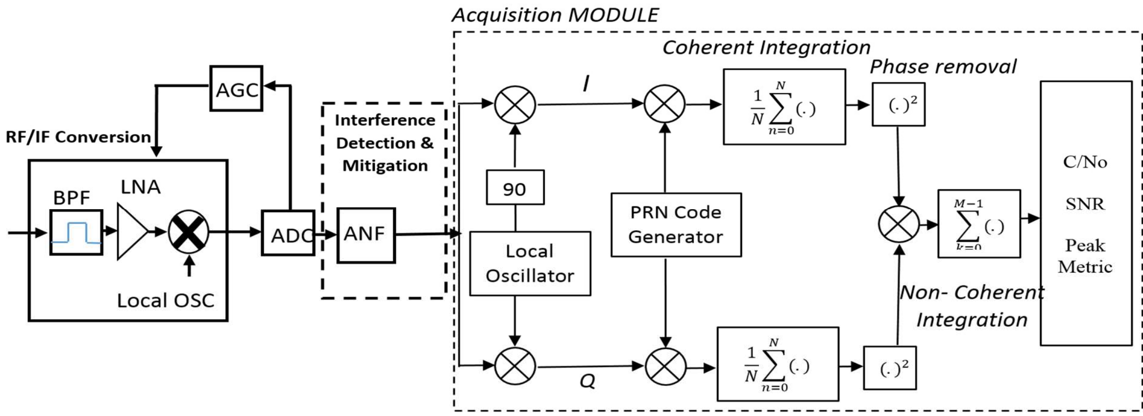

Figure 1.Generic RF/IF and Acquisition module of GPS receivers

In this research main focus is chirp signal jamming tracking. Mathematical model of a linear chirp [9] can be express as in (1), where Pc is chirp signal power, fo is the initial frequency of sweep range, uc is the chirp sweep rate as defined as Bc/Tc and $\emptyset c$ is the initial chirp phase. Instantaneous angular frequency of the chirp signal is calculated by taking the first derivative of phase as shown in (2). Similarly, we can modify (1) to generate a non-linear chirp signal whose instantaneous frequency changes quadratic and cubically expressed as in (3).

$$\frac{\partial}{\partial(nT_s)}\left(\theta[n]\right) = 2\pi f_o + 2\pi u_c nT_s \quad (2)$$

$$j_{chirp}[n] = \sqrt{2P_c}\cos\left(2\pi f_o nT_s + \frac{2\pi u_g (nT_s)^{1+p}}{1+p} + \emptyset_c\right) \quad (3)$$

$$u_g = B_c/T_c^p \quad (4)$$

where p presents the order of the polynomial. For quadratic chirp and cubic chirp p equals 2 and 3 respectively and instantaneous angular frequency for non-linear chirp signal is given by

$$\frac{\partial}{\partial(nT_s)}\left(\theta[n]\right) = 2\pi f_o + \frac{(1+p)\times 2\pi u_c (nT_s)^p}{1+p} \quad (5)$$

B. Received GPS Signal and Acquisition

The ideal GPS L1 signal received along with chirp-type interference can be expressed as in (6) where $s_k[n]$ is transmitted signal by k^{th} satellite, $\eta[n]$ is the thermal noise level and $j_{chirp}[n]$ is the desired chirp interference signal.

$$r[n] = \sum_{k=1}^{N} s_k[n] + \eta[n] + j_{chirp}[n] \quad (6)$$

$$s[n] = \sqrt{2P_i} D_k[n-\tau_k] C_k[n-\tau_k]\cos(2\pi f_{L1+d} nT_s + \delta_i) \quad (7)$$

In (7) theP_i is the signal power, D_k is the navigation data bit of k^{th} satellite with a chip rate of 50 Hz, and C_k is coarse C/A code of k^{th}satellite running at a chip rate of 1.023MHz and τ_k is the code phase delay of k^{th} satellite. Frequency parameter f_{L1+d} represents the L1 carrier frequency with a Doppler shift of f_d (where the sum of these two frequency components results in$f_{L1+d} = f_{L1} \pm f_d = 1575.42MHz \pm f_d$). Next step is the acquisition of the GPS L1 signal which is one of the most critical stages for any GNSS receiver. In Fig .1 a simplified figure of initial stages of GNSS receivers is shown. GPS L1 signal is filtered and down-converted to Intermediate Frequency (IF) where the equivalent filter bandwidth equals B_{IF}.Then IF signal transforms into a sequence of samples by Analog-to-Digital Converter (ADC) controlled by Automatic Gain Control (AGC) unit. The received signal at the IF section is formulated by (8). Parallel code search based acquisition scheme is employed here, in which all the local C/A codes are searched simultaneously.

$$r_{IF}[n] = \sum_{k=1}^{N} s_{kIF}[n] + \eta_{IF}[n] + j_{chirpIF}[n] \quad (8)$$

In parallel code search, the Fourier transform of the local C/A code $c_L[n]$ is performed as in (9) and then the complex conjugate of the Fourier transform of the C/A code is multiplied with the Fourier transform of the received signal $r_{IF}[n]$. The resultant output is then transformed back into the time domain by the inverse Fourier transform. The final output thus represents the correlation between the received signal and the local C/A code known as Cross Ambiguity Function (CAF) as in (9).

$$S(\tau_0, f_d) = \left|\frac{1}{N}\sum_{n=0}^{N-1} r_{IF}[n] c_L[n-\tau_0] e^{-j2\pi f_d}\right|^2 \quad (9)$$

In an ideal scenario after evaluation of CAF, it should present with well-defined sharp peak and the values of the peak corresponds to the value of τ_0 *and* f_d which matches with the delay and Doppler frequency of the satellite in space.

C. Performance Metrics

The performance of the GPS acquisition systems is evaluated using CAF which in the discrete-time domain, can be defined as (9) and the Signal-to-Noise Ratio (SNR) in CAF is calculated by (10). On the other hand, the SNR is simply evaluated by dividing the difference of maximum correlation peak and mean noise

$$SNR(dB) = 10log\left[\frac{\max[S(\tau_0, f_d)] - mean[S(\tau_0, f_d)]}{s.t.d[S(\tau_0, f_d)]}\right] (10)$$

of the search space by the standard deviation of the search space[11]. Second performance metric that is used is called search-grid peak metric α_{peak}, which is simply the ratio between the highest peak and second high peak in search-grid as in (11). If the α_{peak} value is above 2 it means received signal $r_{IF}[n]$ is easily acquirable [11].

$$\alpha_{peak} = \frac{|\max-\text{peak}[S(\tau_0, f_d)]|}{second-\text{peak}\ (|S_{noise\ floor}|)} > 2 (11)$$

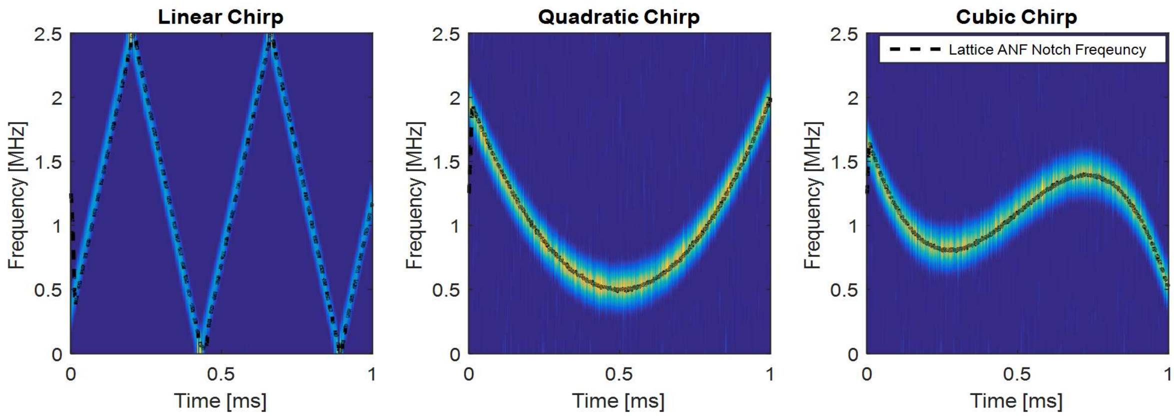

Figure 2.Time-Frequency representation of GPS L1 signal interfered by linear, quadratic and cubic Chirp over 1ms (1 complete C/A code).Black dashed line represents the instantaneous frequency of lattice based ANF

III. ADAPTIVE NOTCH FILTERS

There is an extensive literature on the detection and mitigation of CWI in GNSS. The ANF is the adapts the notch centre frequency creating a narrow notch at the corresponding interference frequency to excise the interference signal. Two candidates for ANF algorithms are modelled and investigated in this section which are lattice based ANF [10] and other on 2nd order direct form IIR ANF [6]. In an adaptive IIR lattice structure the notch filter transfer function from input $x_{in}[n]$ to notch output $y_L[n]$ is expressed as by (12)

$$H_L(z) = \frac{1+\rho}{2}\frac{1-2\beta[n]z^{-1}+z^{-2}}{1-\beta[n](1+\rho)z^{-1}+\rho z^{-2}} \tag{12}$$

$$\beta[n] = \beta[n-1] - \mu.y_L[n](1-\rho)x[n-1] \tag{13}$$

where $\beta$is the notch centre frequency parameter and ρ is notch bandwidth parameter of the lattice notch filter. Update equation for β is given by (13), where μ is fixed step-size and kept fixed rather than time-varying step-size as in [10] to simplify realisation of the algorithm. Direct form 2nd ANF is modelled as given in [6]. The Normalized Least Mean Square (NLMS) algorithm is utilized to update the location of the instantaneous frequency of chirp interference. The transfer function of the notch filter is given as follows

$$H_{notch}(z) = \frac{(1-2Real(z_0)z^{-1}+|z_0|^2z^{-2})}{1-2k_\alpha Real(z_0)z^{-1}+{k_\alpha}^2|z_0|^2z^{-2}} \tag{14}$$

where k_α is the notch bandwidth parameter and z_0 is the notch location on the unit circle corresponds to instantaneous frequency of chirp signal. Output of the ANF is minimized by taking the derivative of (14) with respect to the parameter z_0.The expression of the stochastic gradient is given by

$$grad(C[n]) = -4x_0[n](z_0[n-1]x_e[n-2] - x_e[n-1]) \tag{15}$$

where $x_0[n]$ is the output of Auto-Regressive (AR) is part of the filter and $x_e[n]$ is the output of Moving-Average (MA) part of the filter [9] and the equation to update the zero of ANF becomes as follows

$$z_0[n] = z_0[n-1] + \mu_n \times x_0[n]grad(C[n]) \tag{16}$$

where μ_n normalized step-size. The performance of both ANFs depend on notch bandwidth parameters (ρ &k_α) and fast convergence (μ &μ_n) capability. These parameters play an essential role to track fast variations in frequency and needed to be tuned very carefully. Setting notch bandwidth parameters close to unity (very narrow notch) will preserve the useful signal but it will become difficult for ANF to track fast variations of instantaneous frequency of chirp interference, hence a good trade-off is required to successfully track the frequency varying signal.

Table 1. Simulation Setup

Simulation Parameters		Values
GPS L1 IF signal	Sampling Frequency (F_s)	5MHz
	Intermediate Frequency (IF)	1.25Mhz
	Received Signal Power (P_i)	-160dBW
Acquisition	Front-end Bandwidth (B_{IF})	5MHz
	Coherent Integration Time	1ms
	Doppler bin size	125Hz
Lattice ANF	Step-size (μ)	0.01-0.03
	Notch bandwidth (ρ)	0.85
Direct Form ANF	Step-size (μ_n)	0.01-0.025
	Notch bandwidth (k_α)	0.85

IV. SIMULATION RESULTS

Two digital chirp interference signals are simulated according to definition of the parameters that are explained in Section II and combined with simulated GPS L1 signal modelled in Fig. 1. A complete list of simulation parameters are listed in Table 1. Fig 3 shows time-frequency representation of the simulated GPS L1 signal added with chirp interference signals. Blacked dashed line shows the change of the notch centre frequency of lattice based ANF over time. It is assumed that the generated sweep range of the chirp signal is bounded by the bandwidth of the RF front-end. Also Jamming-to-Nosie Density (J/N_0) range kept is small (between 5dB and 15dB) to make sure that minimal adjustments are required for the update of the adaptive parameters of both ANFs without pushing ANF into unstable region. Additionally the notch bandwidth parameter are kept the same for both ANFs which is 0.85. By doing so, both filters have the same notch bandwidth and are not close to unity. Tracking and convergence of two ANFs are shown in Fig.3. From this simulation it is evident that the variance in the estimated frequency by direct form ANF is more visible near DC and Nyquist as shown by grey line in Fig 3. On other hand, variance of the estimated frequency by Lattice ANF is small and more uniform in nature over a wider frequency range. This is due to fact frequency response of direct form IIR ANF deform and in pass-band unity gain is scaled near

Table 2 : SNR and α_{peak} values at the output of Acquisition module

	Lattice ANF				**Direct Form 2nd order ANF**			
	Linear Chirp		Quadratic Chirp		Linear Chirp		Quadratic Chirp	
J/N_0**(dB)**	**SNR(dB)**	α_{peak}	**SNR(dB)**	α_{peak}	**SNR(dB)**	α_{peak}	**SNR(dB)**	α_{peak}
5	13.87	2.71	14.17	2.87	12.51	2.23	12.73	2.33
8	13.18	2.53	12.96	2.39	11.41	2.01	11.10	2.09
12	12.73	2.31	10.78	2.1	10.47	**1.94**	**9.31**	**1.54**
15	11.93	2.07	10.19	**1.89**	**8.91**	**1.37**	**8.46**	**1.37**

Nyquist and DC region, whereas for Lattice ANF the frequency response maintain it shapes remains close to unity in Nyqusit and DC region. Table 2 lists the resulting values of the performance metrics discussed in Section II. At the output of acquisition module, the values of SNR and α_{peak} are calculated for different power levels of linear and quadratic chirp interference signal. Bold values in Table 2 shows where each of the ANF failed to acquire signal and both SNR and α_{peak} values degrade more prominently for direct form ANF. As long as the SNR at the output of acquisition module is more than 10 dB, the GPS L1 signal is acquirable by employing multiple non-coherent integration over period of 1msec and if the peak value is 2 or more, this means useful signal is more prominent in CAF.

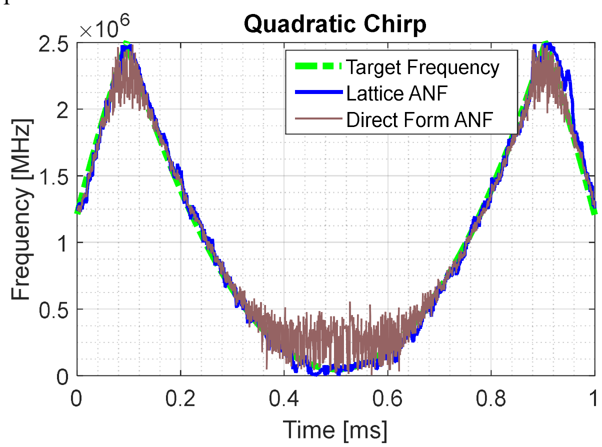

Figure 3. Tracking and converges performance of lattice ANF shown by blue line and Direct Form ANF shown by grey. Green thick dash line represents the target frequency

V. CONCLUSION

In this research article, two different types of chirp jamming signal, the linear and quadratic chirps are modelled and analysed. Using a practical simulation model, a complete GPS L1 IF signal and acquisition module is simulated. Both ANF structures are compared and assessed in terms of tracking, variance of estimated frequency, SNR and α_{peak} for GPS L1 signal. Simulation results prove that the lattice structure shows superior performance in terms of tracking ability and SNR at the output of the acquisition module. Experiment results show that the lattice based ANF is a favourable choice for tracking quadratic and cubic chirps for GPS specific applications. It is well known fact that ~90% of GPS L1 signal power is in the main lobe (2MHz in bandwidth) and furthermore if a portion of this main lobe is discarded, without stopping the GPS L1 being acquired, it would be possible the ANF to excise the interference even faster. As a future study the authors are currently carrying on to find the right trade-off between the quality of interference excision and computational complexity of the system bearing this fact in mind.

REFERENCES

[1] P. Wang, E. Cetin, A. G. Dempster, Y. Wang, and S. Wu, 'Improved Characterization of GNSS Jammers Using Short-Term Time-Frequency Rényi Entropy', *IEEE Transactions on Aerospace and Electronic Systems*, vol. 54, no. 4, pp. 1918–1930, Aug. 2018

[2] M. G. Amin, D. Borio, Y. D. Zhang, and L. Galleani, 'Time-Frequency Analysis for GNSSs: From interference mitigation to system monitoring', *IEEE Signal Processing Magazine*, vol. 34, no. 5, pp. 85–95, Sep. 2017

[3] L. Musumeci, J. T. Curran, and F. Dovis, "A Comparative Analysis of Adaptive Notch Filtering and Wavelet Mitigation against Jammers Interference," *Institute Of Navigation*, vol. 63, no. 4, pp. 533–550, Dec. 2016.

[4] Q. Lv and H. Qin, "A Novel Algorithm for Adaptive Notch Filter to Detect and Mitigate the CWI for GNSS Receivers, " in *2018 IEEE 3rd International Conference on Signal and Image Processing (ICSIP)*, Jul. 2018, pp. 444–451

[5] E. Falletti, M. T. Gamba, and M. Pini, 'Design and Analysis of Activation Strategies for Adaptive Notch Filters to Suppress GNSS Jamming', *IEEE Transactions on Aerospace and Electronic Systems*, (Early Access) pp. 1–1, 2020,

[6] D. Borio, L. Camoriano, and L. L. Presti, "Two-Pole and Multi-Pole Notch Filters: a Computationally Effective Solution for Interference Detection and Mitigation," in *2007 7th International Conference on Telecommunications*, 2007, pp. 1–6.

[7] Y.-E. Chen, Y.-R. Chien, and H.-W. Tsao, 'Chirp-Like Jamming Mitigation for GPS Receivers Using Wavelet-Packet-Transform-Assisted Adaptive Filters', in *International Computer Symposium (ICS)*, Dec. 2016, pp. 458–461

[8] D. Borio, 'Swept GNSS jamming mitigation through pulse blanking', in *2016 European Navigation Conference (ENC)*, May 2016, pp. 1–8

[9] J. R. Klauder, A. C. Price, S. Darlington, and W. J. Albersheim, 'The theory and design of chirp radars', *The Bell System Technical Journal*, vol. 39, no. 4, pp. 745–808, Jul. 1960

[10] Y. R. Chien, "Design of GPS Anti-Jamming Systems Using Adaptive Notch Filters," *IEEE Systems Journal*, vol. 9, no. 2, pp. 451–460, Jun. 2015.

[11] S. W. Arif, A. Coskun, and I. Kale, 'A Fully Adaptive Lattice-based Notch Filter for Mitigation of Interference in GPS', in *2019 15th Conference on Ph.D Research in Microelectronics and Electronics (PRIME)*, Jul. 2019, pp. 217–220